Surface waves at an interface of two metamaterial structures with interelement coupling

A. Radkovskaya,[1] E. Tatartschuk,[2] O. Sydoruk,[3] E. Shamonina,[2,*] C. J. Stevens,[4] D. J. Edwards,[4] and L. Solymar[3]
[1]*Erlangen Graduate School in Advanced Optical Technologies, University of Erlangen–Nuremberg, Paul-Gordan Str. 6, D-91052 Erlangen, Germany*
[2]*Magnetism Division, Faculty of Physics, M. V. Lomonosov Moscow State University, Leninskie Gory, Moscow 119992, Russia*
[3]*Optical and Semiconductor Devices Group, Electrical and Electronic Engineering (EEE) Department, Imperial College, Exhibition Road, London SW7 2BT, United Kingdom*
[4]*Department of Engineering Science, University of Oxford, Parks Road, OX1 3PJ Oxford, United Kingdom*
(Received 8 March 2010; published 28 July 2010)

A configuration of two strongly coupled homogeneous two-dimensional metamaterial lattices of resonant elements is shown to be able to propagate surface magnetoinductive waves along the interface by virtue of coupling between the elements at the boundary. A study of the dispersion equations reveals the existence of two separate pass bands for surface waves which may partly overlap with pass bands supporting bulk waves. Experiments are reported on a structure consisting of 90 magnetically coupled capacitively loaded resonant rings designed to operate around 55 MHz. The measured current distributions and dispersion curves extracted from the experimental data are compared both with numerical simulations, using the generalized Kirchhoff's equation and with analytical expressions derived on the assumption of nearest-neighbor interaction. Excellent agreement between the three approaches is found. Considering that surface waves of various kinds have found a wide range of applications in the past, it is envisaged that this surface wave will open up fresh possibilities. A number of examples are presented. It is conjectured that other existing metamaterial structures might also be suitable candidates for propagating analogous surface waves.

DOI: 10.1103/PhysRevB.82.045430 PACS number(s): 41.20.Jb, 42.25.Bs, 42.70.Qs, 73.20.Mf

I. INTRODUCTION

Waves over surfaces of finite conductivity have been known for over a century.[1,2] They have had great significance in understanding and making possible free space radio transmission in the long and medium wave bands. Dielectric coated metal wires, also capable of supporting surface waves, were used in microwave applications as transmission lines.[3,4] Surface acoustic waves found application in a wide variety of devices (see, e.g., Ref. 5). Perhaps the best known surface waves are that which propagate along the boundary of metals and dielectrics, known originally as surface plasma waves,[6] later called surface plasmons[7] and surface plasmon polaritons.[8] These waves exist due to the negative effective dielectric constant of metals below the plasma frequency. Their properties have been widely investigated (see, e.g., Ref. 9). A proposal for the amplification of surface plasmons has also been made[10] and corroborated by experiment.[11] Optical phonons may also support surface waves[12,13] due to the negative effective dielectric constant available in the range between the longitudinal and transverse optical-phonon frequencies.

Waves due to coupling between metamaterial elements were introduced by Shamonina *et al.*[14] in 2002 who observed that a chain of split-ring resonators[15,16] was capable of supporting slow waves. They called them magnetoinductive (MI) waves. Many aspects of these waves have by now been explored such as the dispersion characteristics of forward and backward waves,[17,18] Brillouin diagrams accounting for evanescent waves,[19] spatial resonances,[20] positive and negative refraction,[21] propagation,[22] waveguide components,[23,24] coupling between the elements,[25] biperiodic structures,[26–28] ring structures,[29] imaging,[30–33] nonlinear effects,[34–37] and retardation.[38,39]

All the experimental studies in the papers quoted above were conducted in the megahertz and gigahertz regions. New impetus to the study of MI waves came a few years later when three new groups (those of X. Zhang, M. Wegener, and H. Giessen) joined in extending the studies to infrared and optical frequencies and to the third dimension. They also introduced new terminology referring to these waves as magnetic plasmons and magnetization waves. Zhang's group studied in more detail the properties of two coupled elements and introduced new structures.[40–44] They also made the interesting proposal that waves due to coupling might also lead to extraordinary optical transmission.[45] Giessen's and Wegener's groups investigated both two-dimensional (2D) and three-dimensional (3D) configurations and, in particular, the fishnet structure.[46–52] Another new direction was initiated by Baena *et al.*[53] and Radkovskaya *et al.*[54] who combined effective-medium theories with those describing MI waves. For a detailed review of waves on coupled elements see Chaps. 7 and 8 in Ref. 55.

Surface waves have several advantages relative to bulk waves: (i) they can concentrate the fields in a region close to the surface, (ii) the surface is available and easily accessible for placing devices, (iii) radiation effects are much reduced in slow waves, (iv) as slow waves, they are capable of interacting with other slow waves and since the advent of metamaterials we also know that (v) their excitation on opposite surfaces of a slab makes possible the operation of the "perfect lens."[56] There is a prospect therefore that combining the versatility of MI waves and their availability in the frequency region from megahertz to optical frequencies with the wide range of applications offered by surface waves that different opportunities for practical applications will be opened.

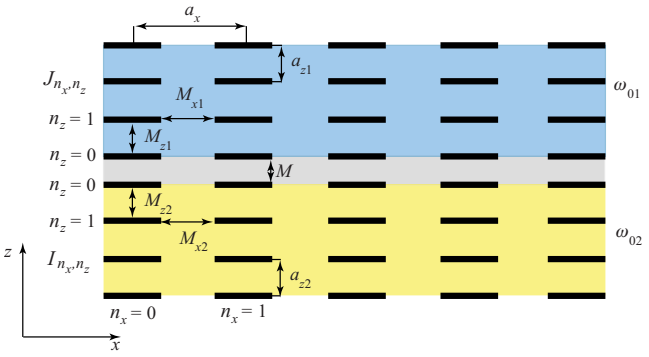

FIG. 1. (Color online) Schematic representation of two coupled lattices capable of propagating MI waves.

Most waves that exist in the bulk have surface-wave counterparts. However, it is far from obvious that MI waves will display a surface wave behavior. In the present paper, we show that two coupled media, each capable of supporting a bulk MI wave in isolation, are indeed able to propagate surface MI waves along their common boundary.

In Sec. II we shall derive the dispersion relations for two strongly coupled homogeneous 2D lattices and in Sec. III establish the conditions under which a wave can propagate along the boundary and decay in the direction transverse to the boundary. In Sec IV we present some examples of dispersion curves showing that at the same frequency it is possible for both surface waves and bulk waves to propagate. Section V describes the experimental apparatus and the experimental arrangement. Experimental results are discussed in Sec. VI. In Sec. VII the experimental results are compared with simulated results obtained from the generalized Kirchhoff's equation. The dispersion curves analytically derived from the nearest-neighbor interaction assumption are compared in Sec. VIII with those derived from experiments and simulations. A discussion on the merits of this type of surface wave is given in Sec. IX and conclusions are drawn in Sec. X.

II. DISPERSION RELATIONS FOR TWO COUPLED LATTICES

The first thought that comes to mind when considering surface waves is that will a medium, that can support bulk waves, also be able to support surface waves along the boundary between the medium and a dielectric? This is obviously not true in general but may be true if one of the media has a negative materials constant (permittivity or permeability). In this paper we adopted a more general approach in our search for surface waves. Instead of an interface between the MI-wave-supporting medium and a dielectric we chose an interface between two media (see Fig. 1) each of them capable of propagating bulk MI waves separately.

We shall now derive the dispersion relation of MI waves in the two adjoining lattices shown in Fig. 1. This problem has already been treated by Syms *et al.*[21] when deriving reflection and transmission coefficients for a wave incident from one of the media. The technique is to find the dispersion relations in the two media separately and then find the coupling between them by writing Kirchhoff's equation for each of the two boundary layers taking into account the mutual inductance between elements across the boundary. In the present paper we have an analogous approach starting with the Lagrangian.[43]

The elements chosen are split-ring resonators, arranged in a planar-axial configuration (Fig. 1). The split-ring resonators are in the x-z plane coupled axially in the z direction. In the experiments they are realized by copper rings loaded by lumped capacitors (see Sec. V) so they can be regarded as LC circuits but, of course, the analysis would be valid for any homogeneous set of resonant elements. The essential requirement is that a_x, which is the period in the x direction, must be the same for both lattices. There is, however, a considerable amount of freedom: the elements can have different separations in the z direction, a_{z1} and a_{z2}, different mutual inductances, M_{x1}, M_{x2}, M_{z1}, and M_{z2}, in the x and z directions, and different resonant frequencies, ω_{01} and ω_{02}. For the existence of surface waves, as it will be shown later, the most important parameter is M, the mutual inductance between the elements across the boundary. The column and row numbers are denoted by n_x and n_z. The currents in the top and bottom lattices are taken as J_{n_x,n_z} and I_{n_x,n_z}, respectively.

The Lagrangian for the upper lattice may be written as follows:

$$\mathcal{L}^{(1)} = \sum_{n_x,n_z} \left\{ \frac{L}{2}[\dot{q}^{(1)}_{n_x,n_z}]^2 - \frac{1}{2C_1}[q^{(1)}_{n_x,n_z}]^2 + M_{x1}\dot{q}^{(1)}_{n_x,n_z} \times (\dot{q}^{(1)}_{n_x-1,n_z} + \dot{q}^{(1)}_{n_x+1,n_z}) + M_{z1}\dot{q}^{(1)}_{n_x,n_z}(\dot{q}^{(1)}_{n_x,n_z-1} + \dot{q}^{(1)}_{n_x,n_z+1}) \right\}, \tag{1}$$

where $q^{(1)}_{n_x,n_z}$ is the charge on the capacitor in element (n_x,n_z), C_1 is the capacitance, L is the inductance, and the dot denotes the time derivative. The superscript (1) refers to the upper lattice. The summation runs from $n_x=0$ to N_x-1 and from $n_z=0$ to N_z-1, where N_x and N_z are the number of elements in the x and z direction, respectively.

The Lagrangian for the lower lattice is also given by Eq. (1) provided the superscript 1 is replaced by superscript 2. When we write the Lagrangian for the interface layers we have to take into account the fact that the two lattices are coupled by the mutual inductance, M. Therefore, the Lagrangians for the interface layers are

$$\mathcal{L}^{(1)}_b = \mathcal{L}^{(1)}(n_x,0) + \dot{q}^{(1)}_{n_x,0}[M\dot{q}^{(2)}_{n_x,0} - M_{z1}\dot{q}^{(1)}_{n_x,-1}],$$

$$\mathcal{L}^{(2)}_b = \mathcal{L}^{(2)}(n_x,0) + \dot{q}^{(2)}_{n_x,0}[M\dot{q}^{(1)}_{n_x,0} - M_{z2}\dot{q}^{(2)}_{n_x,-1}]. \tag{2}$$

Equations (1) and (2) may be converted into differential equations with the aid of the Euler equation (see, e.g., Ref. 43). For the two lattices the operations to be performed are

$$\frac{d}{dt}\left(\frac{\partial \mathcal{L}^{(p)}}{\partial \dot{q}^{(p)}_{n_x,n_z}}\right) - \frac{\partial \mathcal{L}^{(p)}}{\partial q^{(p)}_{n_x,n_z}} = 0 \quad p = 1,2 \tag{3}$$

and for the two boundary layers

$$\frac{d}{dt}\left(\frac{\partial \mathcal{L}_{\mathrm{b}}^{(p)}}{\partial \dot{q}_{n_x,0}^{(p)}}\right) - \frac{\partial \mathcal{L}_{\mathrm{b}}^{(p)}}{\partial q_{n_x,0}^{(p)}} = 0 \quad p = 1,2. \tag{4}$$

Assuming a time variation $\exp(-i\omega t)$ and performing the operations indicated in Eqs. (3) and (4) we have a set of difference equations in terms of the currents

$$J_{n_x,n_z} = -i\omega q_{n_x,n_z}^{(1)} \quad \text{and} \quad I_{n_x,n_z} = -i\omega q_{n_x,n_z}^{(2)}. \tag{5}$$

This set of difference equations may also be obtained by the alternative method of using Kirchhoff's voltage equations. The next step is to assume a wave solution in the form

$$J_{n_x,n_z} = J_0 \exp[i(n_x k_x a_x + n_z k_{z1} a_{z1})],$$

$$I_{n_x,n_z} = I_0 \exp[i(n_x k_x a_x + n_z k_{z2} a_{z2})], \tag{6}$$

where J_0 and I_0 are constants, $k_x a_x$ and $k_{z1,2} a_{z1,2}$ are the phase changes per element in the x and z directions, respectively.

Solving the difference equations with the aid of Eq. (6), we obtain the dispersion equations (the relationship between frequency and wave numbers k_x and k_z) for the upper and lower lattices as follows:

$$1 - \frac{\omega_{01}^2}{\omega^2} + \kappa_{x1}\cos(k_x a_x) + \kappa_{z1}\cos(k_{z1} a_{z1}) = 0,$$

$$1 - \frac{\omega_{02}^2}{\omega^2} + \kappa_{x2}\cos(k_x a_x) + \kappa_{z2}\cos(k_{z2} a_{z2}) = 0, \tag{7}$$

where $\kappa_{x1,2} = 2M_{x1,2}/L$ and $\kappa_{z1,2} = 2M_{z1,2}/L$ are the coupling coefficients, $\omega_{01}^2 = 1/LC_1$ and $\omega_{02}^2 = 1/LC_2$ are the resonant frequencies.

The influence of the boundary layers upon the solution is obtained from Eqs. (2) and (4) in the form

$$\left[1 - \frac{\omega_{01}^2}{\omega^2} + \kappa_{x1}\cos(k_x a_x) + \frac{\kappa_{z1}}{2}\exp(ik_{z1} a_{z1})\right] J_0 + \frac{\kappa}{2} I_0 = 0,$$

$$\left[1 - \frac{\omega_{02}^2}{\omega^2} + \kappa_{x2}\cos(k_x a_x) + \frac{\kappa_{z2}}{2}\exp(ik_{z2} a_{z2})\right] I_0 + \frac{\kappa}{2} J_0 = 0, \tag{8}$$

where $\kappa = 2M/L$. With the aid of Eq. (7), Eq. (8) reduces to

$$-\frac{\kappa_{z1}}{2}\exp(-ik_{z1} a_{z1}) J_0 + \frac{\kappa}{2} I_0 = 0,$$

$$-\frac{\kappa_{z2}}{2}\exp(-ik_{z2} a_{z2}) I_0 + \frac{\kappa}{2} J_0 = 0. \tag{9}$$

The above equation has nontrivial solutions when

$$\exp(-ik_{z1} a_{z1} - ik_{z2} a_{z2}) = \frac{\kappa^2}{\kappa_{z1}\kappa_{z2}}. \tag{10}$$

We now have three equations, the two dispersion equations for the upper and lower lattices and Eq. (10) describing the coupling between them. Our aim is to deduce from them the full dispersion diagram, the dependence of frequency on $k_x a_x$.

III. CONDITIONS FOR SURFACE WAVES

Up to now the analysis has been entirely general, valid for both propagating and evanescent waves. We shall now explore the conditions under which surface waves can be present. In order to be able to talk about waves decaying away from the boundary both k_{z1} and k_{z2} must have imaginary components and considering the form in which the currents are assumed [see Eq. (6)] those imaginary components must be negative. The key equation is Eq. (10). Clearly, in order to satisfy this k_{z1} and k_{z2} must be complex. Introducing $k_{z1,2} = k'_{z1,2} + ik''_{z1,2}$ Eq. (10) can be rewritten as

$$\exp[-i(k'_{z1} a_{z1} + k'_{z2} a_{z2})]\exp[(k''_{z1} a_{z1} + k''_{z2} a_{z2})] = \gamma, \tag{11}$$

where $\gamma = \kappa^2/(\kappa_{z1}\kappa_{z2})$. Surface waves must decay in the transverse direction. There are actually two ways in which they can decay, monotonically or alternately. For monotonic and alternate decay the phase change per element must be zero and π, respectively. It may be seen from Eq. (11) that the right-hand side is a real number and the second exponent always gives us a real positive number. Hence the first exponent must also give a real number depending on the sign of γ. If $\gamma < 0$ (i.e., M_{z1} and M_{z2} are of the opposite sign) then one of the waves must be monotonic and the other one alternate. If $\gamma > 0$ then both waves must have the same type of decay, either monotonic or alternate.

The condition for the existence of surface waves may then be clearly seen from Eq. (11). As mentioned before $k''_{z1} a_{z1}$ and $k''_{z2} a_{z2}$ must both be positive and that can only be true if $|\gamma| > 1$ or

$$M^2 > |M_{z1} M_{z2}|. \tag{12}$$

IV. DISPERSION CURVES

Let us next investigate the role of the various parameters in shaping the dispersion curves. For simplicity let us start with the case when the two lattices are identical, i.e., $\omega_{01} = \omega_{02}$, $M_{z1} = M_{z2}$, $M_{x1} = M_{x2}$, and $a_{z1} = a_{z2}$. In this case condition (12) makes very good sense. The coupling between the lattices must be stronger than the transverse coupling between the elements in the lattices. It is interesting that there are no other conditions. Under usual surface-wave conditions (as it applies both to surface plasmons and surface phonons) the two adjoining media must be different, one of the dielectric constants must be positive and the other one negative. This is not the case for magnetoinductive waves: the two adjoining media can be identical. What matters is the strong coupling between them. Obviously, for the surface waves in the case of identical media the decay rates away from the boundary in the $+z$ and $-z$ directions must be the identical, and also the decay types must be the same: both monotonic or both alternate. Then from Eq. (10) we find for the decay rate

$$k''_{z1} a_{z1} = k''_{z2} a_{z2} = k''_z a_z = \log\frac{|M|}{|M_z|}, \tag{13}$$

whence the dispersion relation takes the form

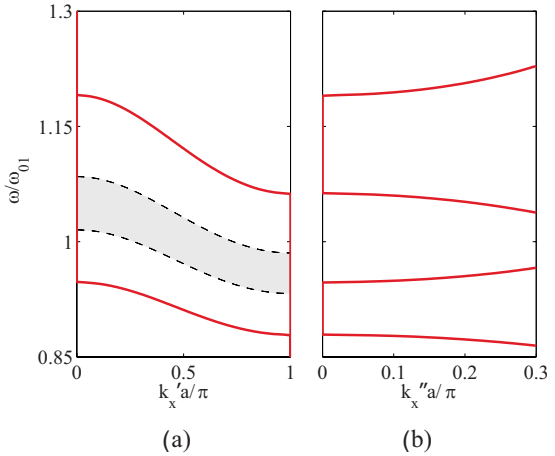

FIG. 2. (Color online) Dispersion curves for two identical lattices. Surface waves are shown by solid lines. Bulk waves may exist within the shaded region bounded by dashed lines. Parameters are $\kappa=0.4$, $\kappa_x=-0.095$, and $\kappa_z=0.05$. (a) Real part and (b) imaginary part of the normalized complex wave number.

$$1-\frac{\omega_0^2}{\omega^2}+\frac{2M_x}{L}\cos(k_x a_x)\pm\frac{M^2+M_z^2}{LM}=0, \tag{14}$$

where the $\pm$ indicates whether the decay is monotonic or alternate. It is worth noting that Eq. (14) is of the same form as that of a one-dimensional MI wave shifted by $\pm(M^2+M_z^2)/(LM)$. There are, clearly, two pass bands, their separation depends mainly on the parameter M/L. The value of M_x determines the dispersion inside the bands (width of the band, the group velocity and whether we have a forward or a backward wave) whereas M_z influences the decay. The smaller is M_z the larger is the decay [see Eq. (13)].

Let us next plot the solution of Eq. (14) for some realistic values of coupling coefficients: $\kappa=0.4$, $\kappa_x=-0.095$, and $\kappa_z=0.05$ corresponding to the planar-axial configuration shown in Fig. 1. The dispersion curves, ω/ω_{01} as a function of $k_x' a_x$ for propagation and $k_x'' a_x$ for attenuation, are plotted in Fig. 2. The surface waves are shown by solid lines.

There are also bulk MI waves described by Eq. (7). For any particular value of $k_x a_x$ the function $\cos(k_z a_z)$ may take any value between -1 and 1. It follows then that MI waves can propagate within the range of frequencies (shaded area in Fig. 2 between dashed lines)

$$\omega_- < \omega < \omega_+, \tag{15}$$

where $\omega_\pm$ can be determined from the equation

$$\frac{\omega_0^2}{\omega_\pm^2}=1+\frac{2M_x}{L}\cos(k_x a_x)\pm\left|\frac{2M_z}{L}\right|. \tag{16}$$

It may be seen in Fig. 2 that there is a frequency region in which bulk and surface MI waves coexist. This is again different from some of the "traditional" surface waves which propagate in the stop band of the bulk waves. In the metamaterial context, however, such coexistence is known (see Ref. 57). Notice that in Fig. 2 the $k_x a_x$ values for bulk and surface modes are different. In other words the dispersion curves for bulk and surface MI waves do not intersect each other. They represent independent solutions. They are not coupled to each other. However, we cannot exclude the possibility that they might become coupled in the presence of a major discontinuity in the structure.

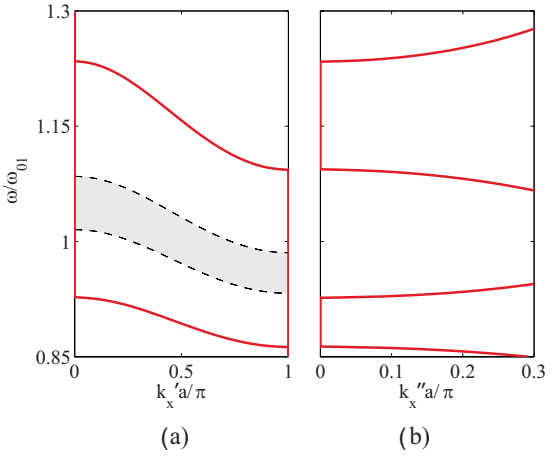

FIG. 3. (Color online) Same as Fig. 2 but the coupling constant between the lattices is increased to $\kappa=0.5$.

The attenuation is plotted only for surface waves and only for the lossless case which we assume here. There is no attenuation in the pass bands and the attenuation sharply increases outside the pass band. If we increase the coupling coefficient between the lattices to 0.5 the two surface wave bands will be further separated and the frequency bands for the bulk and surface waves no longer overlap as shown in Fig. 3.

Next we shall leave the geometry unchanged but assume different resonant frequencies in lattices 1 and 2 choosing $\omega_{02}=1.11\omega_{01}$ (Fig. 4). The dispersion curves plotted show now two pass bands for bulk MI waves (their boundaries are again marked with dashed lines) and the upper and lower pass bands for surface waves. Again the attenuation is plotted only for surface waves.

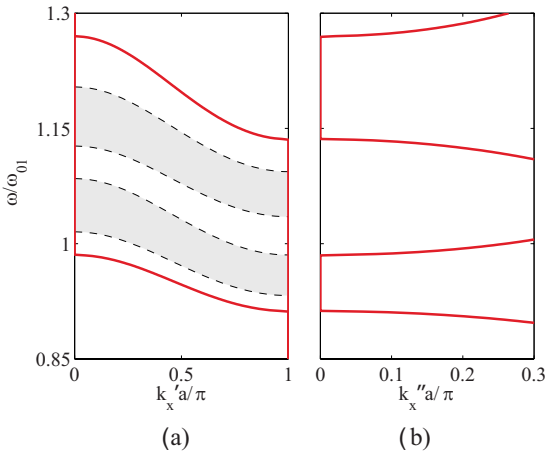

FIG. 4. (Color online) Same as Fig. 2 but resonance frequencies are assumed to be different in the two lattices: $\omega_{02}=1.11\omega_{01}$.

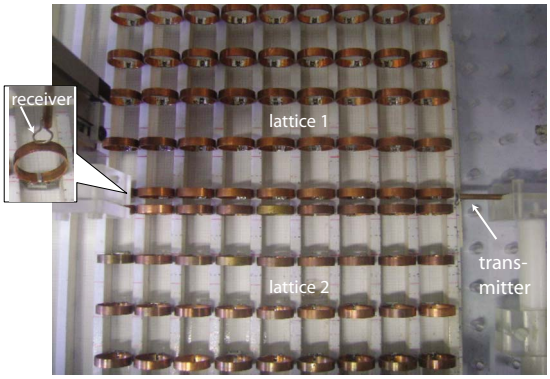

FIG. 5. (Color online) A photograph of the experimental setup. Excitation of the central elements on both sides of the interface by a single transmitting coil may be seen on the right-hand side. Detection is by a receiving antenna moving above the elements.

V. EXPERIMENTAL CONFIGURATION

The experimental arrangement was similar to that reported in Refs. 27 and 32. Two sets of elements were prepared by loading singly split loops (mean radius of 11 mm) by capacitors yielding resonant frequencies of 50.4 and 56 MHz and a quality factor of 165. The elements were arranged on a balsawood to form two adjoining planar-axial lattices of 5 by 9 elements each, with either identical or nonidentical resonant frequencies, and with the distance between the elements variable for each set of measurements. The center-to-center distance between the elements in the planar layers was kept 24 mm in all measurements whereas the distance between layers within each lattice could be varied between 20 and 30 mm. The center-to-center distance across the boundary was only 10 mm assuring the strong coupling needed for the excitation of surface waves.

A photograph (top view) of the adjoining lattices, corresponding to the parameters used in constructing Fig. 4, is shown in Fig. 5. The capacitances, making the rings resonant cannot be seen since they are on the lower side of the rings. The transmitting and receiving antennas are wire coils of 2.5 mm radius connecting the inner and outer conductors of a coaxial cable so that the antenna area is one order of magnitude smaller than that of a split ring. The structure was excited by a transmitter coil put next to the first elements of both interface layers as shown in the photograph, so that the elements were excited asymmetrically, in order to be able to excite both branches of surface modes. The current in each element of the structure was measured by the receiver scanning the magnetic field above the structure (see the inset in the photograph). The phase and amplitude of the signal at each element were determined with the aid of a network analyzer (type HP8753C) at 1601 frequency points between 30 and 78 MHz. The coupling coefficients were measured separately; their values have already been given in the previous section for calculating the theoretical curves.

VI. GENERALIZED KIRCHHOFF'S EQUATIONS METHOD

Current distributions in metamaterial structures of interest can be simulated with the aid of an extremely simple analytical relationship, the generalized Kirchhoff's equation (GKE) introduced for the calculation of currents in Ref. 17. It relates the excitation voltages to the currents via the impedance matrix Z. If there are N elements, in any configuration not necessarily in a regular lattice, then the relationship may be written as

$$\mathbf{V} = \mathbf{ZI}, \tag{17}$$

where

$$\mathbf{V} = (V_1, V_2, \ldots, V_i, \ldots, V_N), \quad \mathbf{I} = (I_1, I_2, \ldots, I_j, \ldots, I_N). \tag{18}$$

Here, V_i is the voltage applied to the ith element and I_j is the current flowing in the jth element. The element Z_{ij} $(i \neq j)$ of the impedance matrix is the mutual impedance between element i and element j. Since $Z_{ij}=Z_{ji}$ the matrix is symmetric. The diagonal elements Z_{ii} give the self-impedance of the ith element equal to

$$Z_{ii} = -i\omega L + \frac{i}{\omega C} + R, \tag{19}$$

where the resistance R is added to account for losses in the elements. For a given excitation the current can be obtained by inverting the $\mathbf{Z}$ matrix. It should be emphasized here that the GKE is a very powerful method. In general, it could take care of the situation in which the coupling between all the elements is of importance. Its disadvantage is that it is a blunt instrument: we can calculate the current distribution but it offers no physical insight. In this sense it is similar to numerical packages, a reason why we prefer to call it simulation rather than theory. In the present case we shall simplify the problem by taking only nearest-neighbor interactions into account.

There are altogether 90 elements in the experiment, hence $N=90$. We shall number them from the upper left-hand corner moving down from 1 to 9 then up to element one in the second column, down to the bottom of the structure, etc. The point and method of excitation has already been described in Sec. V and shown in Fig. 5. In view of the numbering scheme introduced above, V_5 and V_6 are the only elements in the $\mathbf{V}$ vector which are different from zero. The mutual impedances between elements made up by capacitively loaded rings have been calculated before.[27] Thus from the geometry we can determine the $\mathbf{Z}$ matrix and the inversion of the matrix multiplied by the $\mathbf{V}$ vector will yield the current distribution.

VII. CURRENT DISTRIBUTIONS: EXPERIMENT AND SIMULATIONS

The dispersion Eq. (16) illustrated in Figs. 2–4 predicts the existence of various combinations of bulk and surface waves which propagate and/or decay in the two coupled lattices. To verify the dispersion equation we find, both by experiment and by simulations, current distributions which we may compare with each other and with predictions of the dispersion equation.

The technique is to extract the variation in phase and amplitude of the current from the experimental results and com-

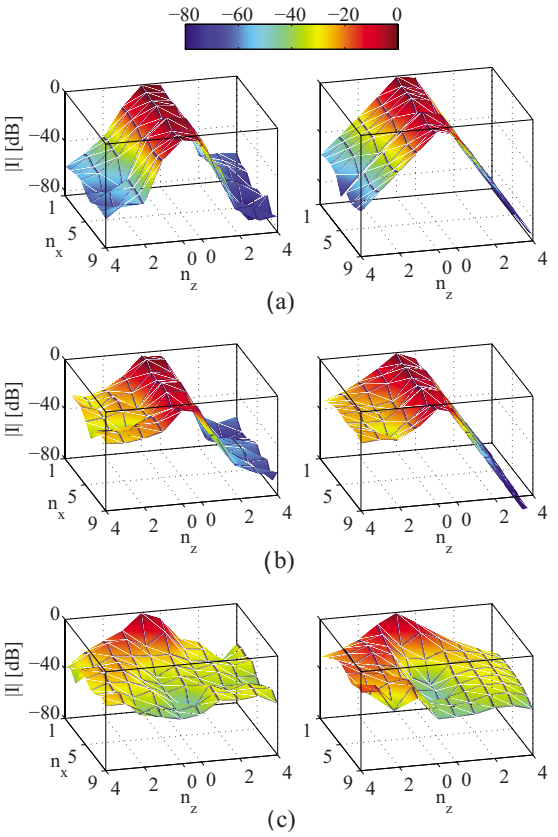

FIG. 6. (Color online) Contour plots of wave amplitudes for nonidentical lattice geometry. Left, measurement; right, simulation. (a) $f=61.59$ MHz. There are no bulk waves, only the surface wave is present in the upper pass band. (b) $f=58.98$ MHz. There is a bulk wave in lattice 2 and there is also a surface wave present in the upper pass band. (c) $f=54$ MHz. There are bulk waves in both lattices. The surface wave is absent.

pare them with the current distributions obtained by the GKE, over a range of frequencies including both pass bands and stop bands of the surface waves for the excitation shown in Fig. 5. We look at a number of examples of both identical and nonidentical adjoining lattices.

In our first example, the adjoining lattices 1 and 2 consist of 5×9 elements having dimensions $a_x=24$ mm, $a_{z1}=a_{z2}=30$ mm. The separation between the boundary layers is 10 mm. The geometry and the resonant frequencies ($f_{01}=50.4$ MHz, $f_{02}=56.0$ MHz) correspond to the dispersion curves plotted in Fig. 4.

The current distributions for three values of the frequency are shown in Figs. 6(a)–6(c) as contour plots: experimental and simulation results are in the left and right columns, respectively, using a logarithmic scale. In the experiments the noise level was quite high so that results plotted below about −50 dB are unreliable. They are shown for completeness but no great significance should be attached to them. Figure 6(a) shows the current distribution at $f=61.59$ MHz in the upper pass band of the surface wave (see the dispersion in Fig. 4). A surface wave is clearly present propagating in the x direction. The decay may be seen to be a little faster for the simulations but otherwise the agreement is very good.

Figure 6(b), plotted at 58.98 MHz, shows the case when, besides the surface wave, bulk waves are also present in

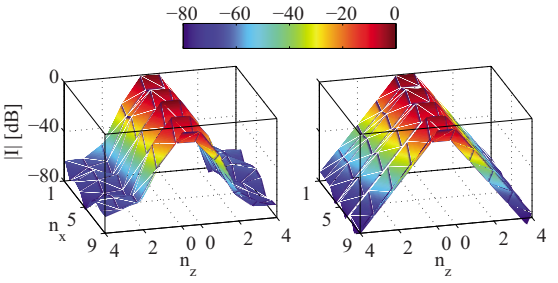

FIG. 7. (Color online) Contour plots of wave amplitudes for identical lattice geometry at $f=59.38$ MHz. There are no bulk waves, only the surface wave is present in the upper pass band. Left, measurement; right, simulation.

lattice 2. The space available for the propagation of bulk waves is rather limited by only four units away from the center. Hence there are numerous reflections from the edges distorting their shape. There is some qualitative agreement between experiment and simulations in the sense that both of them show considerably higher wave amplitudes in lattice 2 than in lattice 1.

At $f=54$ MHz [Fig. 6(c)] the surface wave is no longer there but bulk waves are propagating in both lattices. The waves decay in the x direction as they should due to losses. There is also an indication of reflection from the edge. There is again qualitative agreement between experiment and simulations showing the higher amplitudes in lattice 2. We have done the measurements and performed the simulations for three further frequencies. The agreement between them is about the same as for the higher frequencies and conclusions follow again from the dispersion curves of Fig. 4. At $f=49$ MHz there are both bulk and surface waves, at $f=46.5$ MHz there are only surface waves. At $f=45.5$ MHz both the bulk and surface waves are in the stop band, consequently the currents decay from the point of excitation in all directions.

In further experiments the two resonant frequencies were made equal, $f_{01}=f_{02}=50.4$ MHz, with the separation remaining unchanged. This geometry corresponds to the dispersion curves plotted in Fig. 2. Only one of the results is worth mentioning that is measured at 58.38 MHz (Fig. 7) where the surface wave is in its upper pass band and there are no bulk waves.

VIII. DISPERSION EQUATION DERIVED FROM MEASUREMENTS

Results of the previous section, both experiments and simulations, confirm qualitatively the various combinations of waves which propagate or decay on two adjoining coupled lattices. The qualitative agreement between measured and simulated current distributions both for the case of nonidentical and identical resonant frequencies is remarkably good. A qualitative picture has already emerged from linking Figs. 6 and 7 to the corresponding dispersion equations plotted in Figs. 4 and 2. The theoretical prediction, that surface waves can propagate in a lower and in an upper pass band, has been amply confirmed.

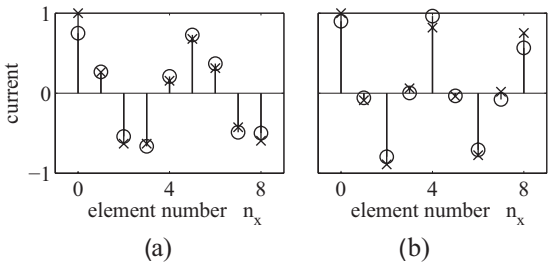

FIG. 8. Variation in the amplitude of the surface wave along the elements. (a) nonidentical lattices at a frequency of 61.59 MHz, (b) identical lattices at a frequency of 58.38 MHz. Circles, measurement; crosses, simulations.

Next we shall show comparisons between experimental and simulated results adding this time losses[17] corresponding to the measured value of the quality factor, $Q=165$. At 61.59 MHz for different resonant frequencies [Fig. 8(a)] and at 58.38 MHz for identical resonant frequencies [Fig. 8(b)] the wave amplitudes are shown by circles for experiments and by crosses for simulations. The agreement is good. The next step is to extract the parameters in the whole frequency region of interest from the kind of plots shown in Fig. 8.

It needs to be noted that since the attenuation is only moderate and we have made no attempts to match the surface waves, they will be reflected at the outer boundary. Hence we shall assume the current in the n_xth element along the boundary in the form

$$I_{n_x} = T_s \exp[\mathrm{i}n_x(k_x a_x)_s] + \Gamma_s \exp[-\mathrm{i}n_x(k_x a_x)_s] + T_b \exp[\mathrm{i}n_x(k_x a_x)_b] + \Gamma_b \exp[-\mathrm{i}n_x(k_x a_x)_b], \quad (20)$$

where T and Γ are the amplitudes of the waves propagating in the $+x$ and $-x$ directions, respectively. The subscripts s and b stand for surface waves and bulk waves. We have now six complex unknowns: T_s, T_b, Γ_s, Γ_b, $(k_x a_x)_s$, and $(k_x a_x)_b$. For any given frequency we can determine them by a simple fitting technique which minimizes the total mean-square deviation between the assumed current [Eq. (20)] and the measured results where again both amplitudes and phases are available. Our primary interest is in $(k_x a_x)_s$, i.e., we wish to reproduce the dispersion equation of the surface waves. The same calculation will also yield $(k_x a_x)_b$ but that is only in effect an overall average of the bulk wave phase shifts.

Knowing the geometry we can find the coupling coefficients. Knowing the coupling coefficients and the quality factor of the individual elements we can plot the dispersion curves. We do this in Figs. 9 and 10 for lattices with nonidentical and identical resonant frequencies already presented in Figs. 4 and 2 for the lossless case. The presentation is also the same. The surface waves are denoted by solid lines, the boundaries of the bulk waves by dashed lines, and the range of bulk waves is shaded. However, we are interested only in the surface waves. The dispersion curves derived from measurements are denoted by dots corresponding to the 1601 discrete frequency values. There are a few spurious dots but the large majority coalesces into a thick continuous curve. The agreement between the theoretical and experimental

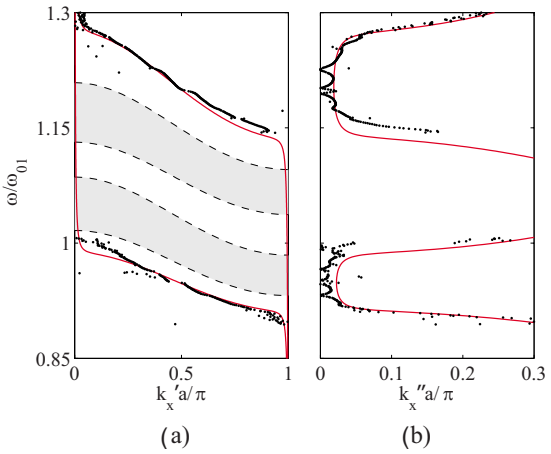

FIG. 9. (Color online) Dispersion curves of surface waves when the lattices have different resonant frequencies. Parameters are the same as for Fig. 4 but losses are included by assuming a quality factor of 165. Theoretical results by solid lines, experimental results by dots which mostly constitute thick continuous lines.

curves is very good both for the real and for the imaginary part of $(k_x a_x)_s$.

IX. DISCUSSION

It has been shown by an analytical theory, simulations, and experiments that surface magnetoinductive waves may exist on magnetically coupled metamaterial structures. The main requirement is strong coupling between adjoining lattices. We have shown that this requirement is satisfied in the structures studied. There is, however, no reason why the same result could not be achieved by other structures. We believe that most metamaterial structures proposed in the past (excluding photonic band-gap materials which do not have resonant elements) would be prominent candidates. We would also make the conjecture that some hybrid structures

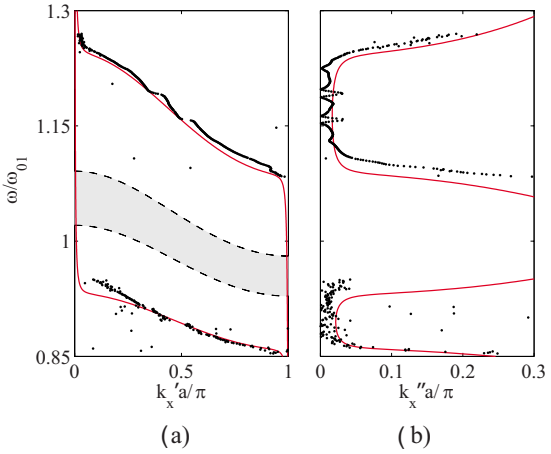

FIG. 10. (Color online) Dispersion curves for the equal-resonant-frequency case. Parameters are the same as for Fig. 2 but losses are included by assuming a quality factor of 165. Theoretical results by solid lines, experimental results by dots which mostly constitute thick continuous lines.

might exhibit surface waves, e.g., a lattice supporting electroinductive waves[58] coupled to a metal-dielectric structure or possibly to a diatomic semiconductor capable of propagating optical phonons.

The surface waves we discussed propagated along a line at the interface of two 2D lattices. Obviously, two strongly coupled 3D structures would also be able to propagate surface waves along the common planar interface. That could give rise to a large number of applications analogously to those achieved by surface acoustic waves and by surface-plasmon polaritons. For example, rearranging the elements on the interface may result in a Fabry-Perot resonator, a Y junction, a directional coupler, or a tunnelling device.

X. CONCLUSIONS

Dispersion curves, showing the existence of a different type of surface wave, belonging to the magnetoinductive wave family, have been derived. The surface waves have been shown to propagate along the boundary of two strongly coupled homogeneous lattices consisting of capacitively loaded rings. A necessary condition for the existence of the surface waves has been formulated analytically. The main requirement is for the coupling between the lattices to be sufficiently strong. Experiments have been conducted on a structure consisting of 90 elements by exciting two boundary elements at one end. The current in each element has been measured and displayed by 3D plots. The amplitude and phase of the surface wave along the boundary has also been plotted. The experimental results for the currents have been compared with those obtained by simulations (solving the generalized Kirchhoff's equations). Excellent agreement has been found for the surface waves and good qualitative agreement for the bulk waves. The theoretical dispersion equation for the surface waves (obtained on the basis of nearest-neighbor interaction) has been compared with that extracted from the experimental current distributions and, again, remarkably good agreement was found. Generalization to other structures has been proposed and potential for applications has been discussed.

ACKNOWLEDGMENTS

A.R. gratefully acknowledges financial support of the Royal Society (Incoming Visitor Scheme); E.T., O.S., and E.S. gratefully acknowledge financial support of the German Research Foundation (SAOT and Emmy Noether-Programme).

*Corresponding author; ekaterina.shamonina@aot.uni-erlangen.de

[1] A. Sommerfeld, Ann. Phys. Chem. **303**, 233 (1899).
[2] J. Zenneck, Ann. Phys. **23**, 846 (1907).
[3] G. Goubau, J. Appl. Phys. **21**, 1119 (1950).
[4] M. King and J. Wiltse, IRE Trans. Antennas Propag. **AP-10**, 246 (1962).
[5] T. E. Parker and G. K. Montress, IEEE Trans. Ultrason. Ferroelectr. Freq. Control **35**, 342 (1988).
[6] A. A. Oliner and T. Tamir, J. Appl. Phys. **33**, 231 (1962).
[7] L. Genzel and T. P. Martin, Surf. Sci. **34**, 33 (1973).
[8] P. Berini, R. Charbonneau, N. Lahoud, and G. Mattiussi, J. Appl. Phys. **98**, 043109 (2005).
[9] S. A. Maier, *Plasmonics: Fundamentals and Applications* (Springer, New York, 2007).
[10] D. J. Bergman and M. I. Stockman, Phys. Rev. Lett. **90**, 027402 (2003).
[11] M. A. Noginov, G. Zhu, A. M. Belgrave, R. Bakker, V. M. Shalaev, E. E. Narimanov, S. Stout, E. Herz, T. Suteewong, and U. Wiesner, Nature (London) **460**, 1110 (2009).
[12] K. L. Kliewer and R. Fuchs, Phys. Rev. **144**, 495 (1966).
[13] N. Marschall and B. Fischer, Phys. Rev. Lett. **28**, 811 (1972).
[14] E. Shamonina, V. A. Kalinin, K. H. Ringhofer, and L. Solymar, Electron. Lett. **38**, 371 (2002).
[15] W. H. Hardy and L. A. Whitehead, Rev. Sci. Instrum. **52**, 213 (1981).
[16] J. B. Pendry, A. J. Holden, D. J. Robbins, and W. J. Stewart, IEEE Trans. Microwave Theory Tech. **47**, 2075 (1999).
[17] E. Shamonina, V. A. Kalinin, K. H. Ringhofer, and L. Solymar, J. Appl. Phys. **92**, 6252 (2002).
[18] M. C. K. Wiltshire, E. Shamonina, I. R. Young, and L. Solymar, Electron. Lett. **39**, 215 (2003).
[19] E. Tatartschuk, A. Radkovskaya, E. Shamonina, and L. Solymar, Phys. Rev. B **81**, 115110 (2010).
[20] O. Zhuromskyy, E. Shamonina, and L. Solymar, Opt. Express **13**, 9299 (2005).
[21] R. R. A. Syms, E. Shamonina, and L. Solymar, Eur. Phys. J. B **46**, 301 (2005).
[22] I. V. Shadrivov, A. N. Reznik, and Y. S. Kivshar, Physica B **394**, 180 (2007).
[23] M. J. Freire, R. Marques, F. Medina, M. A. G. Laso, and F. Martin, Appl. Phys. Lett. **85**, 4439 (2004).
[24] R. R. A. Syms, E. Shamonina, and L. Solymar, IEE Proc. Microwaves, Antennas Propag. **153**, 111 (2006).
[25] F. Hesmer, E. Tatartschuk, O. Zhuromskyy, A. A. Radkovskaya, M. Shamonin, T. Hao, C. J. Stevens, G. Faulkner, D. J. Edwards and E. Shamonina, Phys. Status Solidi B **244**, 1170 (2007).
[26] O. Sydoruk, O. Zhuromskyy, E. Shamonina, and L. Solymar, Appl. Phys. Lett. **87**, 072501 (2005).
[27] O. Sydoruk, A. Radkovskaya, O. Zhuromskyy, E. Shamonina, M. Shamonin, C. J. Stevens, G. Faulkner, D. J. Edwards, and L. Solymar, Phys. Rev. B **73**, 224406 (2006).
[28] A. Radkovskaya, O. Sydoruk, M. Shamonin, E. Shamonina, C. J. Stevens, G. Faulkner, D. J. Edwards, and L. Solymar, IET Microw. Antennas Propag. **1**, 80 (2007).
[29] L. Solymar, O. Zhuromskyy, O. Sydoruk, E. Shamonina, I. R. Young, and R. R. A. Syms, J. Appl. Phys. **99**, 123908 (2006).
[30] M. J. Freire and R. Marques, Appl. Phys. Lett. **86**, 182505 (2005).
[31] M. J. Freire and R. Marques, J. Appl. Phys. **100**, 063105 (2006).
[32] O. Sydoruk, M. Shamonin, A. Radkovskaya, O. Zhuromskyy, E. Shamonina, R. Trautner, C. J. Stevens, G. Faulkner, D. J. Edwards, and L. Solymar, J. Appl. Phys. **101**, 073903 (2007).

[33] M. J. Freire and R. Marques, J. Appl. Phys. **103**, 013115 (2008).
[34] I. V. Shadrivov, A. A. Zharov, N. A. Zharova, and Y. S. Kivshar, Photonics Nanostruct. Fundam. Appl. **4**, 69 (2006).
[35] O. Sydoruk, V. Kalinin, and E. Shamonina, Phys. Status Solidi B **244**, 1176 (2007).
[36] O. Sydoruk, E. Shamonina, and L. Solymar, J. Phys. D **40**, 6879 (2007).
[37] R. R. A. Syms, L. Solymar, and I. R. Young, Metamaterials **2**, 122 (2008).
[38] A. Radkovskaya, M. Shamonin, C. J. Stevens, G. Faulkner, D. J. Edwards, E. Shamonina, and L. Solymar, J. Magn. Magn. Mater. **300**, 29 (2006).
[39] O. Zhuromskyy, O. Sydoruk, E. Shamonina, and L. Solymar, J. Appl. Phys. **106**, 104908 (2009).
[40] H. Liu, D. A. Genov, D. M. Wu, Y. M. Liu, J. M. Steele, C. Sun, S. N. Zhu, and X. Zhang, Phys. Rev. Lett. **97**, 243902 (2006).
[41] Z. Liu, H. Lee, Y. Xiong, C. Sun, and X. Zhang, Science **315**, 1686 (2007).
[42] T. Q. Li, H. Liu, T. Li, S. M. Wang, J. X. Cao, Z. H. Zhu, Z. G. Dong, S. N. Zhu, and X. Zhang, Phys. Rev. B **80**, 115113 (2009).
[43] T. Li, R. X. Ye, C. Li, H. Liu, S. M. Wang, J. X. Cao, S. N. Zhu, and X. Zhang, Opt. Express **17**, 11486 (2009).
[44] H. Liu, Y. M. Liu, T. Li, S. M. Wang, S. N. Zhu, and X. Zhang, Phys. Status Solidi B **246**, 1397 (2009).
[45] H. Liu, T. Li, Q. J. Wang, Z. H. Zhu, S. M. Wang, J. Q. Li, S. N. Zhu, Y. Y. Zhu, and X. Zhang, Phys. Rev. B **79**, 024304 (2009).
[46] G. Dolling, M. Wegener, A. Schädle, S. Burger, and S. Linden, Appl. Phys. Lett. **89**, 231118 (2006).
[47] N. Liu, H. Guo, L. Fu, S. Kaiser, H. Schweizer, and H. Giessen, Adv. Mater. **19**, 3628 (2007).
[48] N. Liu, H. Guo, L. Fu, S. Kaiser, H. Schweizer, and H. Giessen, Nature Mater. **7**, 31 (2008).
[49] N. Liu, S. Kaiser, and H. Giessen, Adv. Mater. **20**, 4521 (2008).
[50] N. Liu, L. W. Fu, S. Kaiser, H. Schweizer, and H. Giessen, Adv. Mater. **20**, 3859 (2008).
[51] M. Decker, S. Linden, and M. Wegener, Opt. Lett. **34**, 1579 (2009).
[52] M. Decker, S. Burger, S. Linden, and M. Wegener, Phys. Rev. B **80**, 193102 (2009).
[53] J. D. Baena, L. Jelinek, R. Marques, and M. Silveirinha, Phys. Rev. A **78**, 013842 (2008).
[54] A. Radkovskaya, E. Tatartschuk, C. J. Stevens, D. J. Edwards, E. Shamonina, and L. Solymar, Congress on Advanced Electromagnetic Materials in Microwaves and Optics Metamaterials'2009, London, 2009.
[55] L. Solymar and E. Shamonina, *Waves in Metamaterials* (Oxford University Press, Oxford, 2009).
[56] J. B. Pendry, Phys. Rev. Lett. **85**, 3966 (2000).
[57] A. Ishikawa, S. Zhang, D. A. Genov, G. Bartal, and X. Zhang, Phys. Rev. Lett. **102**, 043904 (2009).
[58] M. Beruete, M. J. Freire, R. Marques, F. Falcone, and J. D. Baena, Appl. Phys. Lett. **88**, 083503 (2006).